Journal of Magnetism and Magnetic Materials 378 (2015) 246–252

Contents lists available at ScienceDirect

Journal of Magnetism and Magnetic Materials

journal homepage: www.elsevier.com/locate/jmmm

Structural and magnetic characterization and cation distribution of nanocrystalline $Co_xFe_{3-x}O_4$ ferrites

Adel Maher Wahba [a,*], Mohamed Bakr Mohamed [b,c]

[a] Department of Engineering Physics and Mathematics, Faculty of Engineering, Tanta University, Egypt
[b] Physics Department, Taibah University, Al-Madinah Al-Munawara, Saudi Arabia
[c] Ain shams University, Faculty of Science, Physics Department, Cairo, Egypt

ARTICLE INFO

Article history:
Received 25 September 2014
Received in revised form
30 October 2014
Accepted 30 October 2014
Available online 5 November 2014

Keywords:
Autocombustion method
Nanoferrites
Rietveld
Magnetic properties
Cation distribution

ABSTRACT

Structural and magnetic properties have been investigated for $Co_xFe_{3-x}O_4$ nanoferrites ($x=0.5$–1.2, with a step increment of 0.1) prepared by a citrate-precursor autocombustion method. X-ray diffraction patterns (XRD) and Fourier-transform infrared (FTIR) spectra prove the formation of a cubic spinel phase of $CoFe_2O_4$, besides x-dependent $FeCo_2O_4$ spinel for samples with $x \geq 0.7$. Size of the formed nano-crystals ranges from 34 to 45 nm, which is further confirmed with a TEM micrograph. Investigating magnetic parameters such as saturation magnetization, coercivity, and remanence field, through vibrating sample magnetometry (VSM) data, revealed a strong dependence of the magnetic properties of each sample on its own cation distribution being suggested according to the experimental results of XRD, VSM, and IR data.

1. Introduction

Magnetic ferrites in the nanoregime are considered as the field of interest for many researchers due to their enormous applications, including magnetic recording, biomedicine, catalysts, etc. [1]. As a principle, the physical properties of nanoferrites are remarkably different from those of their bulk counterparts. The magnetic properties of any prepared nanoferrite are strongly dependent on the particle size [2], method of preparation [3] and, in addition, on the presence of non-collinear spin structure or local spin canting [4].

The nanoscale spinel ferrite has a face-centered cubic (fcc) structure of the form MFe_2O_4, where M is a divalent atom. The structure contains two interstitial sites occupied by metal cations, namely tetrahedral (A) site and octahedral (B) site. This produces a different local symmetry. The cationic distribution in octahedral and tetrahedral sites is characterized by the inversion parameter γ defined as the fraction of divalent ions in the octahedral sites. The net magnetization, being proportional to the difference between A and B sublattice magnetization, depends on the cationic distribution. In the same manner, since single-ion anisotropy of a specified ion depends on the interstitial site, magnetic anisotropy also depends on the inversion degree. Moreover, several techniques have been used to study the spin-canting phenomenon such as neutron diffraction and ^{57}Fe Mössbauer [5,6]. Results provided evidence that spin canting can be either restricted to a single or extended to both cationic sites.

Cobalt ferrite is a hard magnetic material highly suitable for applications including long-term storage of magnetization. It is characterized by its high cubic magnetocrystalline anisotropy [7]. Magnetic properties of cobalt ferrite could be precisely adjusted by controlling the inversion parameter and the relative presence of Fe^{3+} and Co^{2+} cations in the octahedral site in the ferrite system $Co_xFe_{3-x}O_4$ [8–10]. In this work, the $Co_xFe_{3-x}O_4$ ($0.5 \leq x \leq 1.2$, step 0.1) system has been prepared via citrate-precursor autocombustion method. Structural properties including lattice parameter, crystallite size, XRD density, etc. were analyzed using Rietveld software. The absorption peaks of FTIR data were used to confirm the spinel-phase formation and to trace the variation of the sublattice radii. The dependence of the magnetic properties on the cobalt content and their relation with the presence of canting mechanism in the magnetic moment of Fe^{3+} cations in the B site have also been investigated.

2. Experimental

Nanocrystalline cobalt ferrites with the formula $Co_xFe_{3-x}O_4$ ($x=0.5$–1.2, step 0.1) were prepared by citrate precursor method. Analytical grade metal nitrates $Co(NO_3)_2 \cdot 6H_2O$ and $Fe(NO_3)_3 \cdot 9H_2O$, and dehydrated citric acid $C_6H_8O_7$ were used as starting materials.

---

* Corresponding author.
E-mail address: a_m_wahba@yahoo.co.uk (A.M. Wahba).

http://dx.doi.org/10.1016/j.jmmm.2014.10.164
0304-8853/© 2014 Elsevier B.V. All rights reserved.

The detailed method of preparation is described in a previous work [11]. The autocombustion reaction, reported to occur at nearly 200 °C for cobalt ferrite, produced burnt fluffy ash-like powder. The coarse powder was collected and slightly grounded in a mortar agitate to achieve a fine powder.

To confirm the formation of spinel phase structure, XRD patters of the prepared samples were obtained using a Philips diffractometer (X'pert MPD) with a goniometer using Cu-K_α radiation. The diffracted intensities were collected in the step-scan mode (step size $2\theta=0.015°$, counting time 1.5 s) with the angular range 10–80°. To correct instrumental broadening LaB_6 standard was used. The crystal structure and microstructure were refined applying Rietveld profile method, using MAUD program [12]. Lattice parameter (a) and crystallite size (D) were obtained as results of Rietveld analysis. The XRD density of the prepared samples were calculated from the formula $\rho_{XRD} = 8Mw/N_A a^3$, where the factor 8 indicates the number of formula units in a unit cell, Mw is the molecular weight, N_A is Avogadro's number and a^3 is the cell volume. The powder morphology was recorded by transmission electron microscope (TEM, JEOL JEM-100CX) with accelerating voltage up to 100 kV. Infrared spectroscopy (IR) (Bruker Tensor 27 FTIR Spectrometer) was used in the range of 200–1000 cm^{-1} to confirm the spinel-phase formation and help provide a primary assumption of the cation distribution by tracing the variations of the frequencies of the absorption peaks. For this purpose, quantities of 0.2 mg ferrite per 200 mg KBr were mixed and pressed into pellets. The magnetization, remanence, and the coercive fields data were obtained by tracing M–H hysteresis loops for the powder samples at room temperature using the LDJ vibrating sample magnetometer (VSM) model 9600 with a magnetic field extending up to 20 kOe.

3. Results and discussion

3.1. Structural analysis

XRD patterns of $Co_xFe_{3-x}O_4$ ($x=0.5$–1.2, with a step of 0.1) are shown in Fig. 1. The peaks can be indexed with space group Fd3m to (111), (220), (311), (222), (400), (422), (511) and (440) planes of a cubic unit cell. All XRD patterns were analyzed by using MAUD program that is based on Rietveld method [13]. The Rietveld refinement patterns for $Co_{0.5}Fe_{1.5}O_4$ and $CoFe_2O_4$ are shown in Fig. 2. Samples with $x=0.5$ and 0.6 showed few traces of a second phase of hematite (Fe_2O_3) with percentages of 10% and 2%, respectively. Similar observation was recorded by Bhowmik in his work with bulk $Co_{0.3}Fe_{2.7}O_4$ regardless the method of preparation [14]. All the observed peaks in the XRD patterns of the other samples ($x \geq 0.7$) are located at the Bragg 2θ positions of the spinel phase, which confirm that those samples are single-phase cubic spinel ferrites. The oxygen positions ($x=y=z=u$) were taken as free parameters and all other atomic fractional positions were considered as being fixed. Other parameters such as lattice constants, isothermal parameters, scale factors and shape parameters were considered as free parameters. The sites occupancies distribution in spinel ferrite was obtained from combination of XRD, magnetization and IR data, as we will be seen later. Table 1 illustrates values of D, a, ρ_{XRD}, and oxygen parameter u, for the studied samples. The variation of both the lattice parameter and the XRD density with the cobalt content is shown in Fig. 3. Since the ionic radius of Co^{2+} is larger than that of Fe^{3+} in either A-or B-site, the lattice parameter a is expected to increase monotonically with increasing cobalt content. However, the lattice parameter showed a drop at $x=0.7$ and a slight decrease for $x>1$. This behavior could be explained in terms of the presence of Co^{3+} and Fe^{2+}cations in the prepared samples. This will be explained in detail when discussing the cation distribution and the magnetic properties of the samples. The inverse trend between ρ_{XED} and a in Fig. 3 indicates that the inverse proportion of ρ_{XED} with a^3 dominates its direct proportion with the molar mass M. The sharp drop of the crystallite size at $x=0.7$ (see Table 1) may be attributed to the absence of the phase

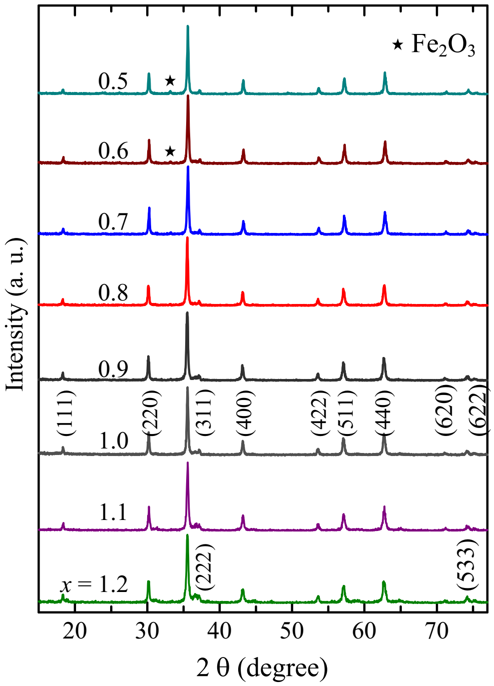

Fig. 1. X-ray powder diffraction pattern for $Co_xFe_{3-x}O_4$ ($0.5 \leq x \leq 1.2$) as-prepared samples.

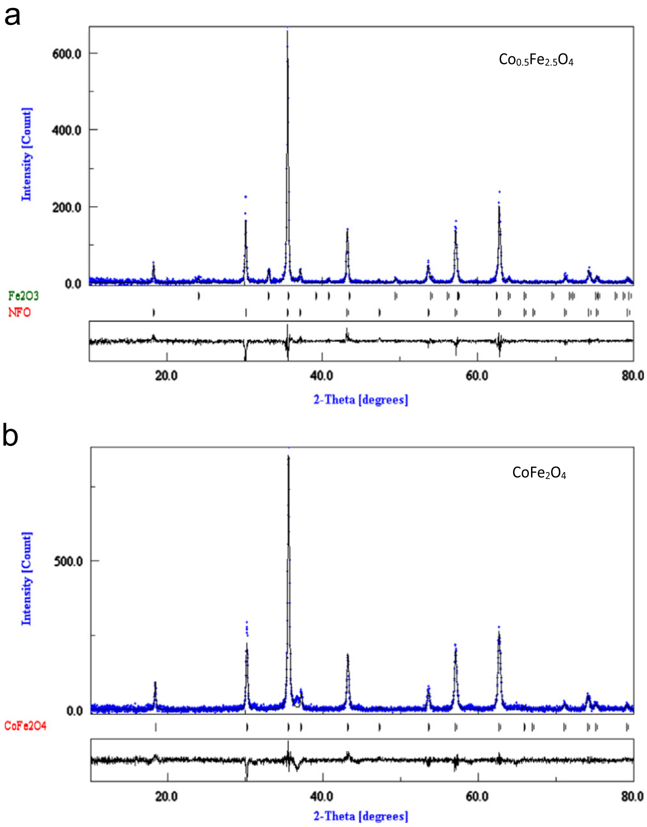

Fig. 2. Rietveld refinement profile for (a) $Co_{0.5}Fe_{2.5}O_4$ and (b) $CoFe_2O_4$ samples.